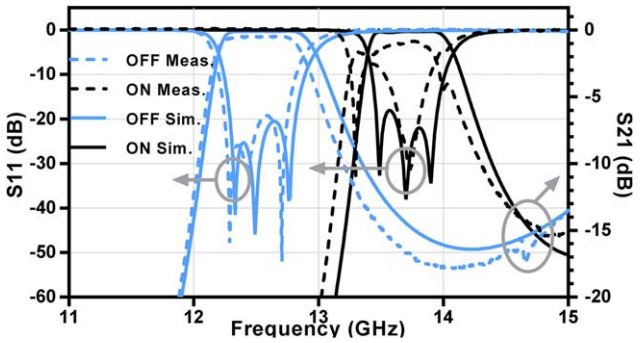

FIGURE 6 Measured *S*-parameters. A, OFF state; B, ON state [Color figure can be viewed at wileyonlinelibrary.com]

practice, Dowel pins can be used to improve alignment, and the PCB width (b) can be slightly widened (eg, 8.2 mm instead of exact 7.9 mm) to improve contact with adjoining waveguide by plated wraps.

Edge plating of multilayer PCBs may suffer from blistered edges which could disconnect the inner metal layers. It has proven to be detrimental for the overall performance. A work-around is to manufacture 3 individual substrate layers (each 1.575-mm thick) with edge plating but without bonding, shown as in Figure 5B. The wraps near the plated edges then become advantageous as they can improve connection for all boards.

4 | CONCLUSION

This article presents a new method of switching high-*Q* bandpass iris filters between 2 states in Ku-band. A tuning range of 1 GHz and equal bandwidths have been achieved. High *Q*-factor of at least 500 is attained by hybrid integration of metal rectangular waveguide for resonators and low loss PCB for the switchable irises.

ACKNOWLEDGMENT

This work was supported through access to the Australian National Fabrication Facility (ANFF) Design House software at the NSW NODE of ANFF.

ORCID

Liang Gong http://orcid.org/0000-0002-3596-3865

REFERENCES

[1] Cameron R, Mansour JR, Kudsia CM. Microwave filters for communication systems: fundamentals. In: *Design and Applications*. Ch. 14.5. Hoboken, NJ: Wiley; 2007: 521–524.

[2] PellicciaCacciamani L, Farinelli FP, Sorrentino R. High-Q tunable waveguide filters using ohmic RF MEMS switches. *IEEE Trans Microwave Theory Tech.* 2015;63:3381–3390.

[3] King Yuk C, Ramer R, Guo YJ. Switchable waveguide iris filter using planar dipoles. Paper presented at: 2013 IEEE MTT-S International Microwave Symposium Digest (IMS); 2013:1–4; Seattle, WA.

[4] Baghchehsaraei Z, Oberhammer J. Parameter analysis of millimeter-wave waveguide switch based on a MEMS-reconfigurable surface. *IEEE Trans Microwave Theory Tech.* 2013;61(12):4396–4406.

[5] Feng X, Ke W. Guided-wave and leakage characteristics of substrate integrated waveguide. *IEEE Trans Microwave Theory Tech.* 2005;53:66–73.

[6] Entesari K, Saghati AP, Sekar V, Armendariz M. Tunable SIW structures: antennas, VCOs, and filters. *IEEE Microwave Mag.* 2015;16(5):34–54.

[7] Mansour RR. UWMEMS Design Handbook (ver. 5) [Online]. 2011.

How to cite this article: Gong L, Chan KY, Ramer R. A third-order bandpass iris filter with reconfigurable dielectric irises. *Microw Opt Technol Lett.* 2018; 60:1287–1290. https://doi.org/10.1002/mop.31154

Received: 21 September 2017

DOI: 10.1002/mop.31153

Planar quasi-isotropic antenna for drone communication

Syed Imran Hussain Shah[1] | **Manos M. Tentzeris**[2] | **Sungjoon Lim**[1]

[1] School of Electrical and Electronics Engineering, Chung-Ang University, Seoul 156-756, Republic of Korea

[2] The School of Electrical and Computer Engineering, Georgia Institute of Technology, Atlanta, Georgia 30332-0250

Correspondence
Manos M. Tentzeris, The School of Electrical and Computer Engineering, Georgia Institute of Technology, Atlanta, Georgia 30332-0250.
Email: etentze@ece.gatech.edu
and
Sungjoon Lim, School of Electrical and Electronics Engineering, Chung-Ang University, Seoul 156-756, Republic of Korea.
Email: sungjoon@cau.ac.kr

Funding information
MSIT (Ministry of Science and ICT), Korea, under the ITRC (Information Technology Research Center) support program, Grant/Award Number: IITP-2017-2012-0-00559; IITP (Institute for Information & communications Technology Promotion)

Abstract

In this article, a planar antenna with quasi-isotropic radiation pattern is proposed for applications in drone

communication. The proposed antenna consists of top-loaded monopole and slotted loop antennas. The top-loaded monopole provides a monopole-like radiation pattern with a planar profile. To compensate for nulls in the monopole radiation pattern, a slotted loop antenna is added. Therefore, when two radiation patterns are combined, a quasi-isotropic pattern is achieved with a low profile thickness of 7.2 mm. The performance of the proposed antenna is verified by simulation and experimental results. The antenna's 10-dB impedance bandwidth is in the range of 2–2.4 GHz. The quasi-isotropic radiation pattern is verified from both simulation and measured results.

KEYWORDS

drone communication, isotropic antenna, loop antenna, monopole antenna, slot antenna

1 | INTRODUCTION

Drones are unmanned radio-controlled aircraft and can fly in the absence of a human pilot on-board. Drones are receiving considerable attention for various applications including, but not limited to, operations in unsafe areas, environmental monitoring and sensing, aerial spreading of fertilizers, and agricultural chemicals, disaster management, and for transportation of goods from one place to another. Drones are radio-controlled; therefore RF communication between the drone and the remote pilot is necessary to control its position and navigate the drone. The two-way communication between drone and operator requires close monitoring and control of the drone's telemetry data and auxiliary sensor data in real time. Without reliable and adaptable communication, unmanned flights would be impossible. Full spatial coverage is required for drone communication; therefore an antenna radiating an isotropic pattern is an attractive choice for unmanned flight. However, antennas that radiate a true isotropic radiation pattern do not exist.[1] Therefore, various three-dimensional antennas with quasi-isotropic radiation patterns have been presented.[1–3] In Ref. [1], a tridimensional quasi-isotropic antenna is designed by combining two slot antennas and a vertical monopole antenna. In Ref. [2], a small spherical antenna is presented as a device that radiates a quasi-isotropic pattern. In Ref. [3], a tridimensional quasi-isotropic antenna is designed by folding a slot antenna. However, three-dimensional antennas are not preferred in some applications. In Refs. [4–6] array antennas are investigated for quasi-isotropic radiation pattern applications. In Ref. [7], a quasi-isotropic antenna is presented using folded split ring resonators. In addition, some low-cost antennas with planar profiles are also investigated for quasi-isotropic radiation pattern applications.[8–11] In Ref. [8], a planar quasi-isotropic antenna is proposed by the combination of two crossed dipoles. In Ref. [9], an inverted-F antenna is used to produce a quasi-isotropic antenna. In Ref. [10], a planar quasi-isotropic antenna is designed by a combination of sequentially rotated L-shaped monopoles. In Ref. [11], a quasi-isotropic antenna is designed by using two bent dipoles for RFID applications. However, the efficiency of this type of antenna is reduced by mounting it on a metallic object.

In this article, a planar antenna that emits a quasi-isotropic radiation pattern is proposed for drone communication applications. The proposed antenna consists of top-loaded monopole and slotted loop antennas. First, the top-loaded monopole is designed which provides monopole-like radiation pattern. Then, the slotted loop antenna is added to compensate for the nulls in the monopole radiation pattern. Therefore, when two radiations are combined, a quasi-isotropic pattern is achieved from an antenna with a planar profile. The performance of the proposed antenna is verified by simulation and experimental results. Its 10-dB impedance bandwidth is in the range of 2–2.4 GHz. The quasi-isotropic radiation pattern is verified from both the simulation and measured results. The proposed antenna is suitable for drone communication, where full spatial coverage is required.

2 | ANTENNA DESIGN

The antenna is designed to emit a quasi-isotropic radiation pattern. First, a top-loaded four-element monopole antenna is designed to emit a monopole-like radiation pattern. Grounded coplanar-waveguide (GCPW) technology is used to design the top-loaded monopole antenna presented in Figure 1A. A monopole-like radiation pattern is achieved because of vertical shorting vias and a circular patch, as this combination provides a horizontal magnetic current distribution. According to the duality theorem, a horizontal magnetic current source is equivalent to an electric current source in a vertical configuration.[12] Therefore, a vertical monopole-like radiation pattern is achieved in a planar structure. The top-loaded monopole antenna has nulls in the z-direction. To compensate for these nulls, a slotted loop is employed on top of the ground plane of the GCPW as shown in Figure 1B. The slotted loop has a total length of one wavelength at an operating frequency of 2.1 GHz. The length (L_2) and width (W_s) of each side of the slotted loop are 64 mm and 1.2 mm, respectively. The slotted loop plays an important role to cover nulls as can be seen from the radiation pattern in Figure 1B. However, a null remains in the $-z$ direction. To compensate for this null, a rectangular slot is designed in the bottom ground plane of the GCPW. After adding the rectangular slot, emitted radiation in the $-z$ direction is increased and the null in this direction is compensated for. The final

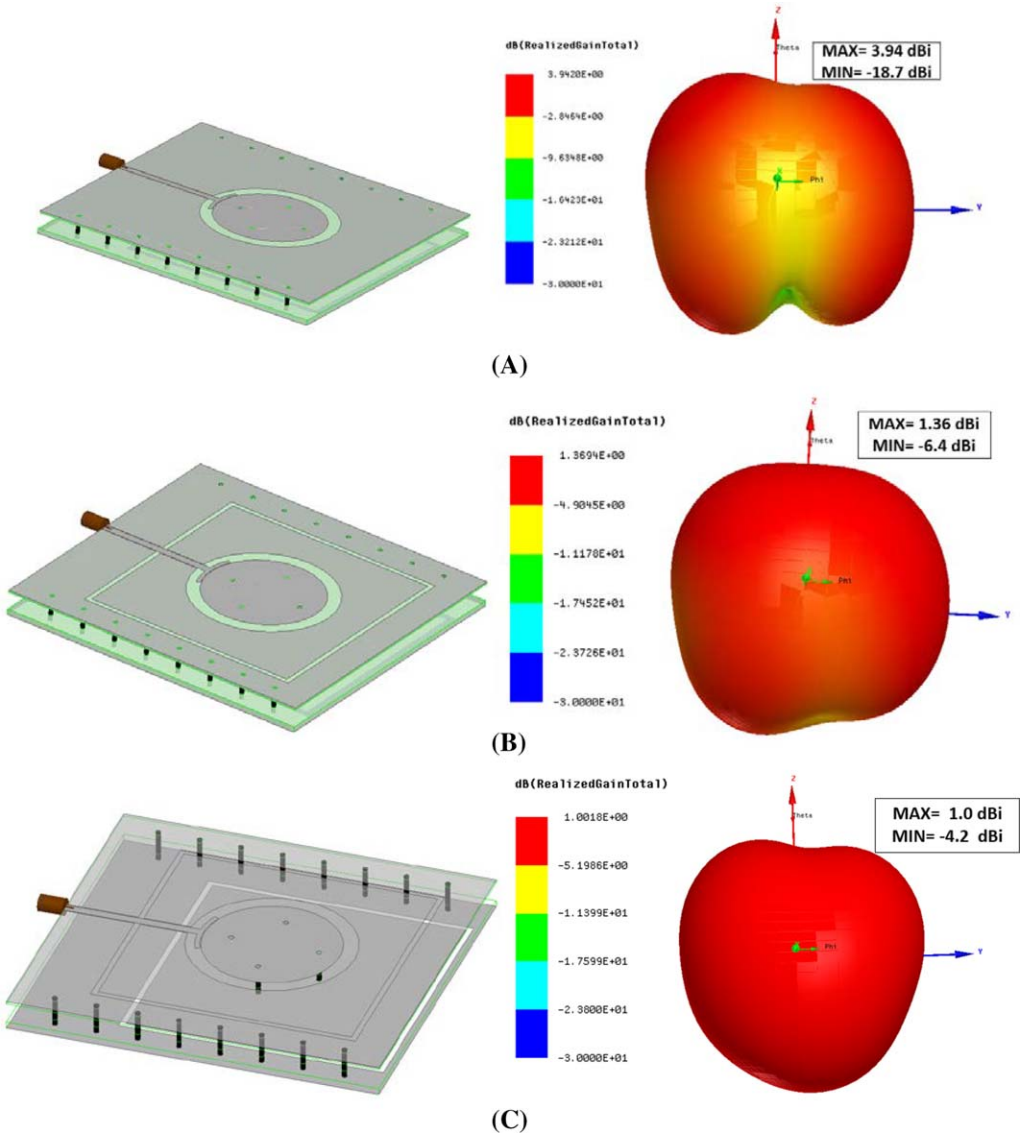

FIGURE 1 Antenna design: (A) top-loaded monopole and its radiation pattern; (B) top-loaded monopole with slotted loop antenna and its radiation pattern; (C) top-loaded monopole with slotted loop on top and bottom ground planes and its radiation pattern [Color figure can be viewed at wileyonlinelibrary.com]

radiation pattern of the top-loaded monopole, with slotted loops on the top and bottom ground planes of the GCPW is shown in Figure 1C. As can be seen from the radiation pattern, there are no nulls in the radiation pattern, hence the proposed antenna emits a quasi-isotropic radiation pattern with full spatial coverage. The proposed antenna is fed power by a 50-Ω transmission line. An arc-shaped matching stub is employed between the transmission line and the circular patch for impedance matching. Parametric study to determine the optimal dimensions of the arc-shaped matching stub and the gap between the circular patch and the stub is performed to obtain correct impedance matching at the desired operation frequency. The process is presented in Figure 2. The optimized length of the arc shaped stub L_s is 11 mm and the optimized gap (G) between the circular patch and arc-shaped stub is 0.2 mm. The geometry of the final top-loaded monopole with slotted loops is presented in Figure 3.

3 | FABRICATION AND MEASUREMENT RESULTS

A prototype of the proposed quasi-isotropic antenna is presented in Figures 3 (antenna layout) and 4 (photos of the prototype). The top-loaded monopole antenna consists of three layers. The top and bottom layers are fabricated on a glass-reinforced epoxy laminate (FR4) substrate, both having dielectric constant and loss tangent of 0.05, respectively. The thicknesses of the top and bottom layers are 0.6 mm (h_1) and 1.6 mm (h_2), respectively. The top layer consists of the

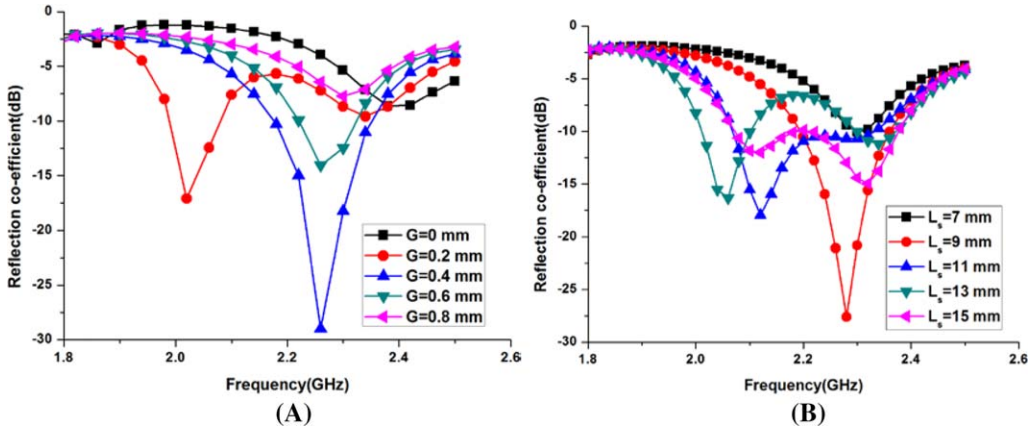

FIGURE 2 Simulated reflection coefficients for (A) various values of G and (B) various values of L_s [Color figure can be viewed at wileyonlinelibrary.com]

feeding network, the circular patch, and the top ground plane. The top surface of the upper FR4 layer and the bottom plane of the lower FR4 layer are made from copper as shown in Figure 3A. The bottom layer consists of a ground plane. The top and bottom layers are separated by an air gap (h_3) of 5 mm. The air gap is employed to increase the 10-dB impedance bandwidth. Silver vias having a diameter of 0.8 mm are used to connect the top and bottom ground planes. The spacing between vias (d_2) is 10 mm. The inner vias (also 0.8 mm) connect the circular patch to the bottom ground plane. The fabricated prototype of the proposed antenna is shown in Figure 4.

The reflection coefficient of the proposed antenna is measured with an Anritsu vector network analyzer. The

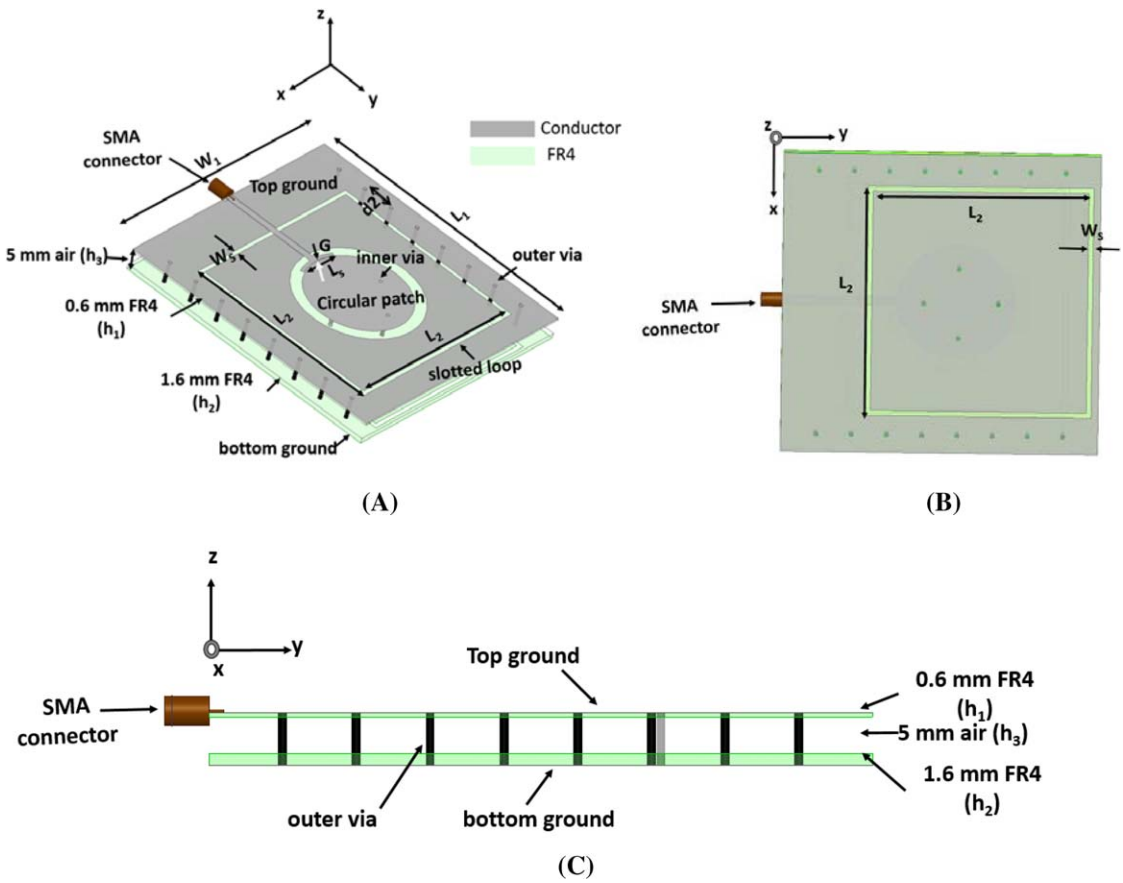

FIGURE 3 Antenna design layout. (A) Antenna design layout front view $L_1 = 90$ mm, $W_1 = 85$ mm, $L_2 = 64$ mm, $W_s = 1.2$ mm; (B) back view; and (C) side view [Color figure can be viewed at wileyonlinelibrary.com]

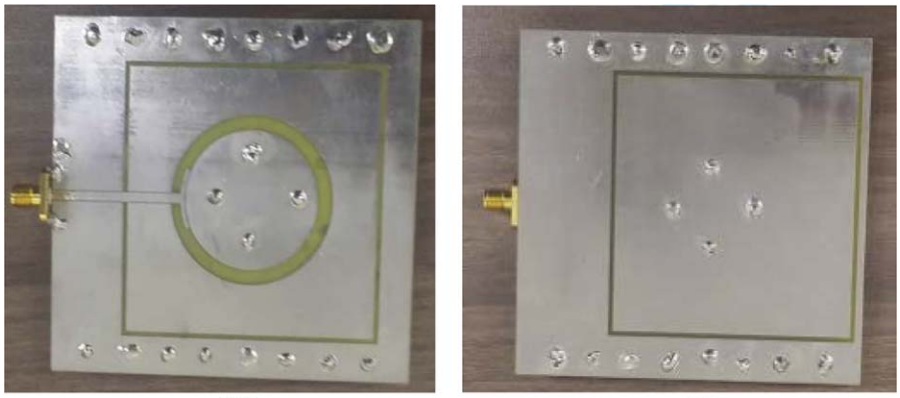

FIGURE 4 Fabricated proposed antenna: (A) front side and (B) back side [Color figure can be viewed at wileyonlinelibrary.com]

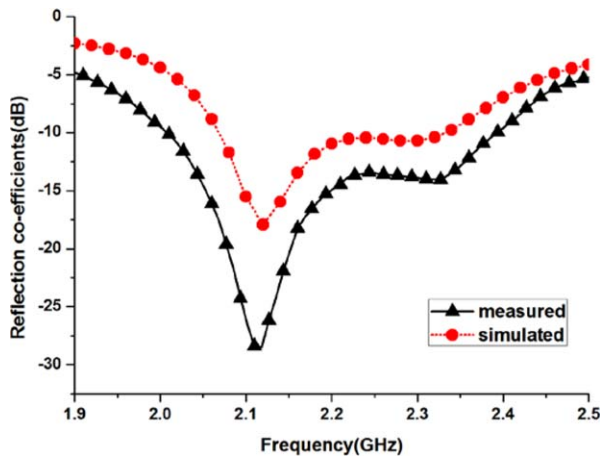

FIGURE 5 Simulated and measured reflection coefficients of the proposed antenna [Color figure can be viewed at wileyonlinelibrary.com]

simulated and measured reflection coefficients are in good agreement and are presented in Figure 5. The antenna shows simulated and measured 10-dB impedance bandwidths of 400 MHz in the range of 2–2.4 GHz (18% bandwidth).

Figure 6 shows the (a) simulated and (b) measured three-dimensional (3D) radiation patterns of the antenna. An anechoic chamber was used as the measurement instrument. As can be seen from the measured 3D radiation pattern, no nulls are present; therefore, the antenna can provide full spatial coverage and can be considered a quasi-isotropic antenna. The antenna has a maximum gain of 2.74 dBi and a minimum gain of −10.22 dBi, therefore gain deviation between maximum and minimum gains in the entire 3D volume is 12.9 dBi. The measured gain deviation is higher than the simulation, which is due to the loss tangent of the FR4 substrate and manufacturing tolerances such as alignment. However, the antenna does provide full spatial coverage and exhibits the characteristics of a quasi-isotropic antenna.

4 | CONCLUSION

A novel planar antenna with quasi-isotropic radiation pattern is proposed. The quasi-isotropic radiation pattern is achieved by a combination of top-loaded monopole and slotted loop antennas. First, the top-loaded monopole is designed to provide a monopole-like radiation pattern. Then, the slotted loops are introduced on the top and bottom ground planes of top-loaded monopole to compensate for the nulls in the monopole radiation pattern. Therefore, a quasi-isotropic pattern is achieved with planar profile antenna, which is suitable

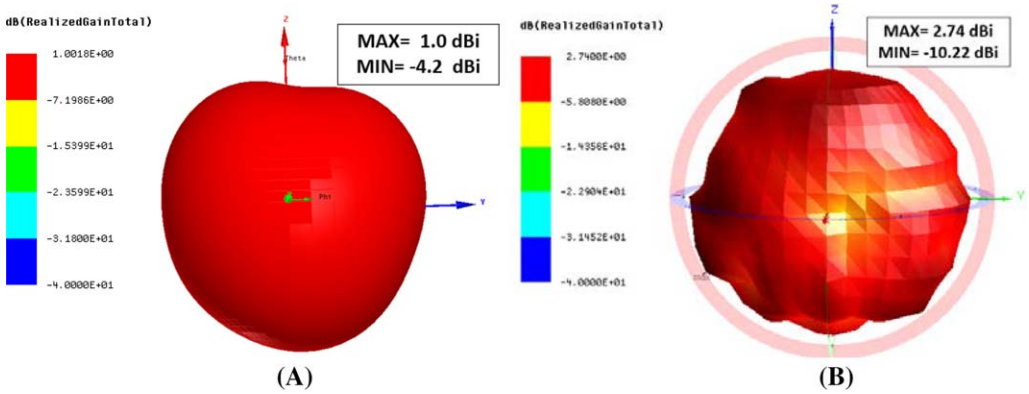

FIGURE 6 3-D radiation pattern at 2.1 GHz: (A) simulated and (B) measured [Color figure can be viewed at wileyonlinelibrary.com]

for drone communication, where full spatial coverage is required. The performance of the proposed antenna is verified using simulation and experimental results. Its 10-dB impedance bandwidth is in the range of 2–2.4 GHz. The antenna's quasi-isotropic radiation pattern is verified from both the simulation and measured results.

ACKNOWLEDGMENTS

This research was supported by Chung-Ang University Research Scholarship Grants in 2016 and the MSIT (Ministry of Science and ICT), Korea, under the ITRC (Information Technology Research Center) support program (IITP-2017-2012-0-00559) supervised by the IITP (Institute for Information & communications Technology Promotion).

ORCID

Sungjoon Lim http://orcid.org/0000-0002-5049-9300

REFERENCES

[1] Long SA. A combination of linear and slot antennas for quasi isotopic coverage. *IEEE Trans Antennas Propag.* 1975;23(4): 572–575.

[2] Mehdipour A, Aliakbarian H, Rashed-Mohassel J. A novel electrically small spherical wire antenna with almost isotropic radiation pattern. *IEEE Antennas Wirel Propag Lett.* 2008;7:396–399.

[3] Deng C, Li Y, Zhang Z, Feng Z. Design of a three-dimensional folded slot antenna with quasi-isotropic radiation pattern. In: IEEE Antennas and Propagation Society, AP-S International Symposium (Digest). October 2015, pp. 588–589.

[4] Psychogiou D, Hesselbarth J. Diversity antennas for isotropic coverage. In: Wireless Technology Conference (EuWIT), 2010 European; 2010, pp. 101–104.

[5] Gazzah H. Optimum antenna arrays for isotropic direction finding. *IEEE Trans Aerosp Electron Syst.* 2011;47(2):1482–1489.

[6] Byun G, Hyun J-C, Seo SM, Choo H. Optimum array configuration to improve the null steering performance for CRPA systems. *J Electromagn Eng Sci.* 2016;16(2):74–79.

[7] Kim JH, Nam S. A compact quasi-isotropic antenna based on folded split-ring resonators. *IEEE Antennas Wirel Propag Lett.* 2017;16:294–297.

[8] PanLi G, Zhang Y, Feng ZZ. Isotropic radiation from a compact planar antenna using two crossed dipoles. *IEEE Antennas Wirel Propag Lett.* 2012;11:1338–1341.

[9] Pazin L, Dyskin A, Leviatan Y. Quasi-Isotropic X-band inverted-F antenna for active RFID tags. *IEEE Antennas Wirel Propag Lett.* 2009;8:27–29.

[10] Deng C, Li Y, Zhang Z, Feng Z. A wideband isotropic radiated planar antenna using sequential rotated l-shaped monopoles. *IEEE Trans Antennas Propag.* 2014;62(3):1461–1464.

[11] Liang L, Member S, Hum SV, Member S. A low-profile antenna with quasi-isotropic pattern for UHF RFID applications. *IEEE Antennas Wirel Propag Lett.* 2013;12:210–213.

[12] Yousaf J, Jung H, Kim K, Nah W. Design, analysis, and equivalent circuit modeling of dual band PIFA using a stub for performance enhancement. *J Electromagn Eng Sci.* 2016;16(3): 169–181.

How to cite this article: Imran Hussain Shah S, Tentzeris MM, Lim S. Planar quasi-isotropic antenna for drone communication. *Microw Opt Technol Lett*. 2018; 60:1290–1295. https://doi.org/10.1002/mop.31153

Received: 27 September 2017

DOI: 10.1002/mop.31152

A low-cost microwave sensing platform for water accumulation abnormality detection in lungs

Mohammed M. Bait-Suwailam | Omar Al-Busaidi | Ahmed Al-Shahimi

Department of Electrical and Computer Engineering, Sultan Qaboos University, Muscat, Oman

Correspondence
Mohammed Bait-Suwailam, Department of Electrical and Computer Engineering, Sultan Qaboos University, Muscat, Oman.
Email: msuwailem@squ.edu.om

Abstract

In this article, water accumulation abnormalities in small-scale lungs are numerically and experimentally studied at microwave regime. The noninvasive passive microwave sensing platform considered here comprises the use of two low-profile patch antennas. The sensors, operating at the ISM band, are attached back-to-back to the skin surface of the lungs. By monitoring the sudden changes of computed transmission coefficient (both magnitude and phase) between the two sensors, qualitative measures can be developed to estimate whether significant water accumulation in lungs take place or not, which can provide further insights at an early medical diagnosis. Several numerical case studies are developed and studied here that mimic various water accumulation scenarios within the modeled lungs. A practical small-scale yet low-cost platform integrated with the microwave sensors was demonstrated and validated. The results correlate reasonably well with numerical results.